Highly confined flow past a stationary circular cylinder

Sachin Saurabh,sachin.saurabh07@gmail.com

Lecturer,Department of mechanical engineering,Assosa University,Ethiopia,8271732022/+251989428048,Sachin.saurabh07@gmail.com

Abstract

A stabilized finite-element formulation incorporating Streamline Upwind/Petrov-Galerkin (SUPG) and Pressure Stabilized/Petrov-Galerkin (PSPG) terms has been used to explore the highly confined (90% blockage) flow of viscous fluid past a stationary circular cylinder. A fully developed inlet velocity profile in conjunction with no-slip side walls has been used for the computations. Results have been presented for Re = 5 to 150 where Re is the Reynolds number based on diameter of cylinder, centreline velocity at inlet and viscosity of fluid. A very interesting result from the current investigation is that the surface pressure is positive along the entire circumference of the cylinder for Re up to 80. A very narrow regime of negative pressure is noted for Re 80. At low Re, such as 5, the magnitude of forward stagnation pressure is of the order of 103, which is significantly higher than the one for unbounded flow. Imposition of blockage also enhances the cylinder drag significantly. At Re = 150, the drag for 90% blockage is about 90 times of its unbounded counterpart. The laminar separation of flow initiates at an Re between 30 and 40. The separation bubble elongates approximately linearly with Re. The transition to unsteady flow takes place within the interval 100< Re <110. For unsteady flow, the phase portraits for drag and lift exhibits symmetry about the zero lift line. The flow is periodic over the unsteady regime. At Re = 150 the flow is periodic with multiple frequencies. The drag-lift phase portrait contains three crossover points and four loops at Re = 150.

Keywords *stabilized finite-element, confined flow, circular cylinder, high blockage*

1. Introduction

Ever since the work done by von-Karman early in last century in the field of fluid mechanics, huge amount of work has been done in this field. In-spite of extensive experimental and numerical studies on flow past a bluff bodies, flow around a circular cylinder at high blockage still remains a challenging problem.As available literature lacks knowledge of such problems. The variation in the flow characteristics due to the lateral walls is seen by various researchers. Tezduyar et al. (1994) investigated the two-dimensional unsteady incompressible flow and reported the effect of lateral boundary of computation domain on different flow parameters. Also the choice of bounded domain gives more specific results of the flow than observed by unbounded case. Laminar1separation Reynolds number, Res, as presented by Dennis et al. (1970) for unconfined motion steady fluid flow to be less than 7. Dennis et al. (1970) used FDM to investigate the flow for Re =5-100 and also stated the wake length variation with Re to be linear. Sen et al. (2009) presented the value of Res to be around 6.29 for B =0.005 and has also presented that there is no effect of blockage on flow parameters for B less than 0.01..

2. The governing equations

2.1 The incompressible flow equations

Let $\Omega \subset \mathrm{IR}^{nsd}$ be the spatial domain, where nsd = 2 is the number of space dimensions and (0,T) be the temporal domain. The boundary of Ω is denoted by Γ and is assumed to be piecewise smooth. The closure of the domain is denoted by $\bar{\Omega}$. The spatial and temporal coordinates are denoted by x and t, respectively. The

equations governing the unsteady flow of an incompressible fluid are:

$$\rho\left(\frac{\partial \mathbf{u}}{\partial t} + \mathbf{u} \cdot \boldsymbol{\nabla}\mathbf{u}\right) - \boldsymbol{\nabla} \cdot \boldsymbol{\sigma} = 0 \qquad \text{on } \Omega \times (0,T), \tag{1}$$

$$\boldsymbol{\nabla} \cdot \mathbf{u} = 0 \qquad \text{on } \Omega \times (0,T). \tag{2}$$

Here u and σσ σ denote the fluid velocity and the Cauchy stress tensor, respectively. The stress is the sum of its isotropic and deviatoric parts:

$$\boldsymbol{\sigma} = -p\mathbf{I} + \mathbf{T}, \quad \mathbf{T} = 2\mu\varepsilon(\mathbf{u}), \quad \varepsilon(\mathbf{u}) = \frac{1}{2}((\boldsymbol{\nabla}\mathbf{u}) + (\boldsymbol{\nabla}\mathbf{u})^T) \tag{3}$$

where p, I, μ and εε ε are the pressure, identity tensor, dynamic viscosity of the fluid and strain rate tensor, respectively. Both, the Dirichlet and Neumann-type boundary conditions are accounted for and are represented as

$$\mathbf{u} = \mathbf{g} \text{ on } \Gamma_g, \quad \mathbf{n} \cdot \boldsymbol{\sigma} = \mathbf{h} \text{ on } \Gamma_h, \tag{4}$$

Γg and Γh are complementary subsets of the boundary Γ, n is its unit normal vector and h is the surface traction vector. The initial condition on the velocity is specified on Ω at t = 0:

$$\mathbf{u}(\mathbf{x},0) = \mathbf{u}_0 \text{ on } \Omega_0, \tag{5}$$

where u0 is divergence-free, i.e. u0 satisfies Equation (2). The momentum equation for steady incompressible flow is obtained by dropping the time-derivative in Equation (1)

3 The finite-element formulation

The spatial domain Ω is discretized into non-overlapping sub-domain Ωe=1,2,.....,nel where nel is the number of elements. Sh uu u and Sh p be the finite dimensional trial function spaces for velocity and pressure, respectively and the corresponding weighting function spaces are denoted by Vh uu u and Vh p . these function spaces are defined

as:

$$\mathcal{S}_{\mathbf{u}}^h = \{\mathbf{u}^h | \mathbf{u}^h \in [H^{1h}(\Omega)]^2, \mathbf{u}^h \doteq \mathbf{g}^h \quad \text{on } \Gamma_g\}, \tag{6}$$

$$\mathcal{V}_{\mathbf{u}}^h = \{\mathbf{w}^h | \mathbf{w}^h \in [H^{1h}(\Omega)]^2, \mathbf{w}^h \doteq 0 \quad \text{on } \Gamma_g\}, \tag{7}$$

$$\mathcal{S}_p^h = \mathcal{V}_p^h = \{q^h | q^h \in H^{1h}(\Omega)\}, \tag{8}$$

$$\text{where } H^{1h} = \{\phi^h | \phi^h \in C^0(\overline{\Omega}), \phi^h \in P^1 \forall \Omega^e\}. \tag{9}$$

Sachin Saurabh

Here, P1 represents the first degree polynomials. Thus, over the element domain, this space is formed by using first degree polynomials in space and time. Globally, the interpolation functions are continuous in space but discontinuous in time. The stabilized space-time formulation for deforming domains is then written as follows:

$$\text{given } (\mathbf{u}^h)_{n^-}, \text{ find } \mathbf{u}^h \in (\mathcal{S}_{\mathbf{u}}^h)_n \text{ and } p^h \in (\mathcal{S}_p^h)_n \text{ such that } \forall \mathbf{w}^h \in (\mathcal{V}_{\mathbf{u}}^h)_n, q^h \in (\mathcal{V}_p^h)_n,$$

$$\int_{\Omega} \mathbf{w}^h \cdot \rho \left(\frac{\partial \mathbf{u}^h}{\partial t} + \mathbf{u}^h \cdot \boldsymbol{\nabla} \mathbf{u}^h - \mathbf{f} \right) d\Omega + \int_{\Omega} \boldsymbol{\varepsilon}(\mathbf{w}^h) : \boldsymbol{\sigma}(p^h, \mathbf{u}^h) d\Omega + \int_{\Omega} q^h \boldsymbol{\nabla} \cdot \mathbf{u}^h d\Omega$$

$$+ \sum_{e=1}^{n_{el}} \int_{\Omega^e} \frac{1}{\rho} \tau \left[\rho \left(\frac{\partial \mathbf{w}^h}{\partial t} + \mathbf{u}^h \cdot \boldsymbol{\nabla} \mathbf{w}^h \right) - \boldsymbol{\nabla} \cdot \boldsymbol{\sigma}(q^h, \mathbf{w}^h) \right] \cdot$$

$$\left[\rho \left(\frac{\partial \mathbf{u}^h}{\partial t} + \mathbf{u}^h \cdot \boldsymbol{\nabla} \mathbf{u}^h - \mathbf{f} \right) - \boldsymbol{\nabla} \cdot \boldsymbol{\sigma}(p^h, \mathbf{u}^h) \right] d\Omega^e$$

$$+ \sum_{e=1}^{n_{el}} \int_{\Omega^e} \delta \boldsymbol{\nabla} \cdot \mathbf{w}^h \rho \boldsymbol{\nabla} \cdot \mathbf{u}^h d\Omega^e$$

$$= \int_{(\tau_n)_h} \mathbf{w}^h \cdot \mathbf{h}^h d\tau \qquad (10)$$

In the variational formulation as given above, the first three terms and the right hand side constitute the Galerkin formulation of the problem. The first series of element level integrals in Equation (10) are the SUPG (streamline-upwind/Petrov-Galerkin) and the PSPG (pressure-stabilizing/Petrov-Galerkin) stabilization terms added to the variational formulations of the momentum and the continuity equations, respectively. At high Re, in an advection dominated flow, the Galerkin formulation of the flow equations lead to node-to-node oscillations in the velocity field. This numerical instability is overcome by adding the SUPG stabilization contribution to all the terms of the Galerkin weak form of the momentum equations. The SUPG formulation for convection dominated flows was introduced by Hughes & Brooks (1979) and Brooks & Hughes (1982). PSPG stabilization terms are added to the formulation to enable the use of equal order interpolation for velocity and pressure.Hughes et al. (1986) introduced the pressure stabilization methods in the context of Stokes flow. This method uses equal order interpolation for velocity and pressure, thus circumvents the Babuska-Brezzi or inf-sup stability condition yet provides stable solutions. Tezduyar et al. (1992c) generalized the method to finite Reynolds number flows and introduced the PSPG term. The PSPG contribution is added to the Galerkin weak form of the continuity equation. This in turn results in a coupled equation system that possesses non-zero coefficients for pressure in the continuity equation, thus bringing definiteness in the matrix system. In the current formulation, τSUPG and τPSPG are equal and represented by the symbol τ. The parameter τ is defined as:

$$\tau_{SUPG} = \tau_{PSPG} = \left[\left(\left(\frac{2\|\mathbf{u}^h\|}{h} \right)^2 + \left(\frac{12\nu}{h^2} \right)^2 \right) \right]^{-0.5} \qquad (11)$$

where h is the characteristic element length. The parameter δ is added to ensure numerical stability at high Reynolds numbers. This is a least squares term based on the continuity equation and is expressed as

$$\delta = \frac{h}{2} |\mathbf{u}^h| z, \qquad (12)$$

Sachin Saurabh

with the following definition of z

$$z = \begin{cases} (\frac{Re_u}{3}) & \text{for} \quad Re_u \leq 3, \\ 1 & \text{for} \quad Re_u > 3 \end{cases} \qquad (13)$$

where, Re_u is the local or element Reynolds number. more details of the semi-discrete finit element formulation can be found in Tezduyar et al. (1992c).

4 Problem description

4.1 Problem set-up

An infinitely long cylinder of Diameter D is placed mid-way between two lateral walls of a channel which are at a distance of H apart, as shown in Figure. The flow characteristics are such that the fluid enters the channel with a parabolic profile (fully developed) and the lateral walls are assigned with no-slip condition on velocity, i.e. the velocity is set to zero at upper and lower boundaries. Neumann condition for velocity is applied on downstream boundary that corresponds to stress-free condition. Re for this fluid is based on the centreline velocity.
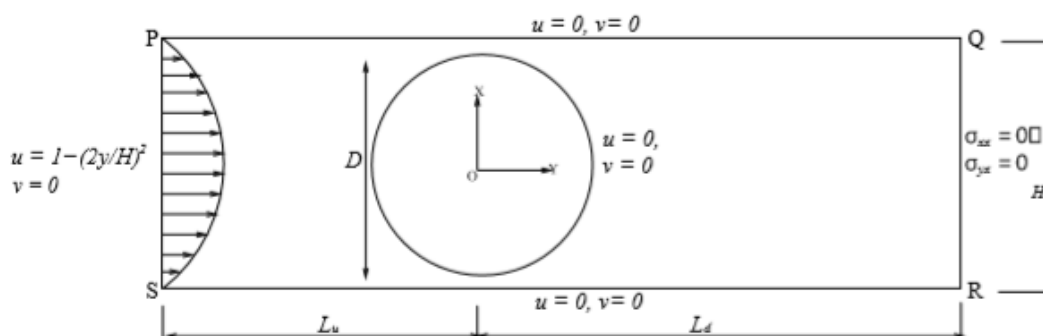

Figure 1: Problem set-up for flow past a circular cylinder at high blockage($B/H = 0.9$).

4.2 The finite-element mesh

A finite-element mesh used for computing the flow around the confined cylinder is shown in Figure 4.2. The distances of the upstream and downstream boundaries from the origin of the cylinder are denoted by Lu and Ld, respectively. In the present work, Lu = 50D and Ld = 100D. The mesh is structured, non-uniform and consists of 90298 nodes and 89504 bilinear quadrilateral elements.
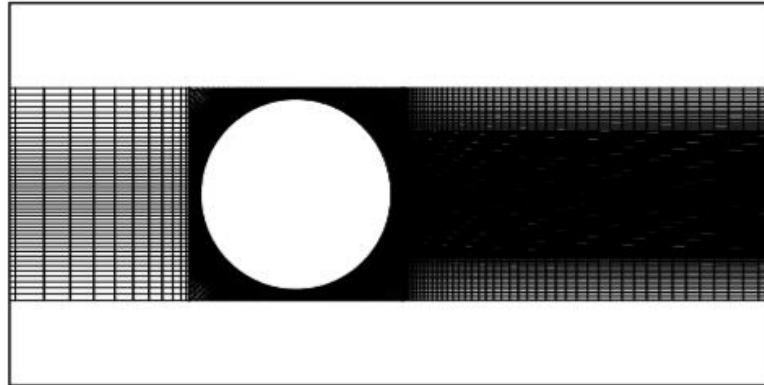
Sachin Saurabh

Figure 2: Finite-element mesh for simulating flow past a circular cylinder at 90% blockage with 90298 nodes and 89504 elements.

5 Results

The present numerical study performed by numerically solving the equations of flow and motion. The results are presented for $5 \leq Re \leq 150$. The computations are done for a two dimensional flow with B = 0.9.

Various post processing tools were used to extract the data from the files generated by FORTRAN code

5.1 Variation of drag and eddy length with Re

Variation of drag and eddy length is shown in figure with Re. It is well known that drag decreases with Re but it is observed that drag is very high at low Re which drastically decreases at higher Re in steady state at high blockage B = 0.9.
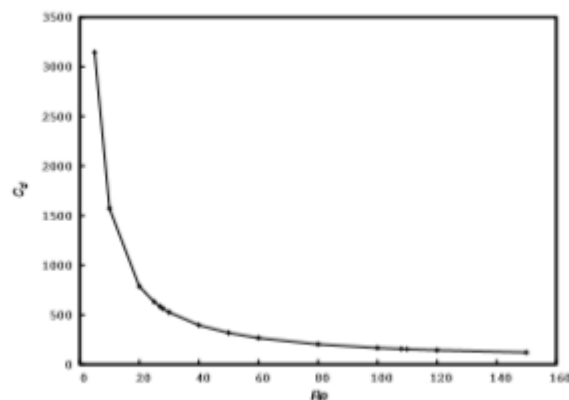

Figure 3: Variation of drag coefficient with Re at blockage of 0.9.

Sachin Saurabh

Eddy length is the streamwise distance between the wake stagnation and rear stagnation point. From observation of streamline contours it is demonstrated that bubble length increases with increase in Re. The change of eddy length with Re for steady flow past a circular cylinder can be establish from figure 4.

5.2 Development of steady separation bubble with Re

Development of the steady separation bubble is determined by streamline contour plots with Re. Streamlines are plotted for range $28 \leq Re \leq 50$. It is observed that no separation bubble is formed for $Re < 30$. The
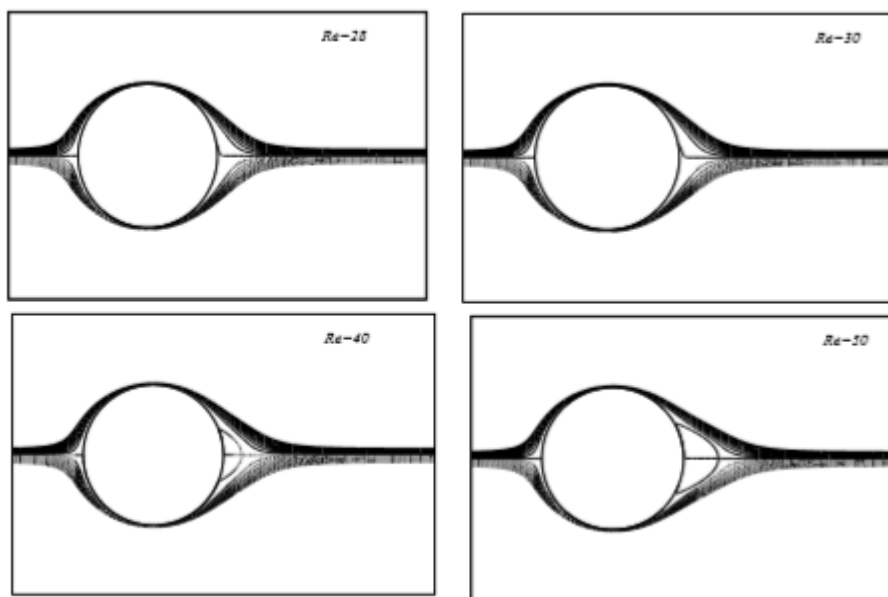
bubble once formed continously enlarges with Re.

Figure 4: Devlopment of steady sepration bubble with Re.

5.3 Surface pressure distribution

Surface pressure distribution is shown in figure from Re = 5-150 for laminar flow past a circular cylinder. The pressure coefficient Cp is computed using no-slip boundary conditions on cylinder surface. It has been observed that large value of surface pressure coefficient exists at low Re. It decreases drastically at angle of 80◦-110◦, after that its value is asymptotic in nature.

The maximum value of surface pressure coefficient lies at forward stagnation point Cpo and at rear stagnation point the value is much smaller. The value of surface pressure coefficient remains positive at all points upto $Re \leq 80$ after this a very narrow regime of negative pressure is noted at $\theta = 100$◦.
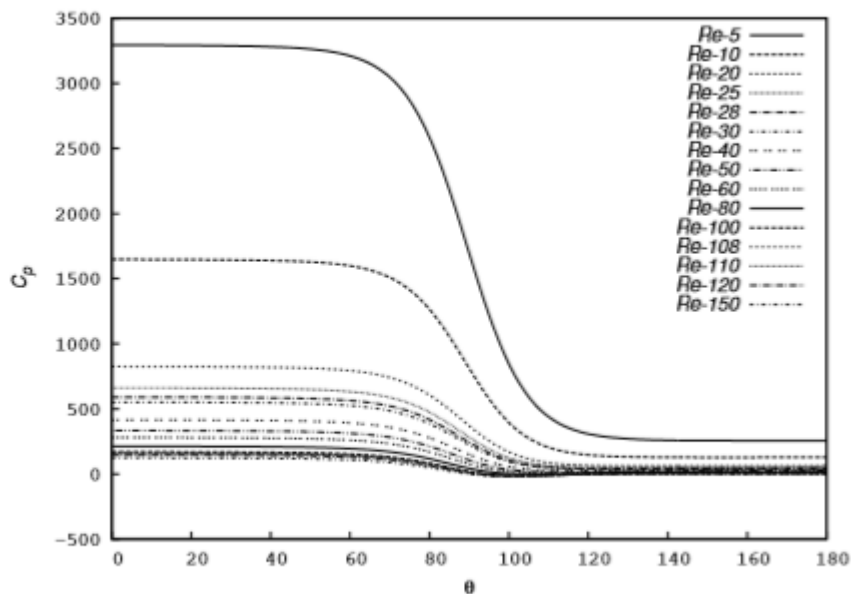
Sachin Saurabh

Figure 5: Pressure distribution along the surface of the cylinder with $\theta°$.

5.4 Onset of unsteadiness

Flow behaviour remains steady at Re = 100, time series of Cd shows the value of drag coefficient with increasing Re, it is observed that the flow is fully steady for Re < 108. At Re = 108, the transition from steady to unsteady flow regime takes place and is marked as critical Re(Rec). For Re > 108, the shedding of vortices initiates.

5.4.1 Vorticity Contours

In highly confined flow the wall separation bubble ahead of the wake stream is also formed. This is due to the boundary effects of the lateral walls which is not the case for unbounded flow. This tells that due to confinement (at Re = 150) size of the standing vortices are reduced and the critical Re of vortex shedding is delayed.

At Re = 150 vorticity contour represents 2S mode of vortex-shedding as two vortices are shed per cycle. One from the top side while the other from the bottom side of cylinder. There is also vortices at the wall due to high blockage and same sign of vortices interact with each other. For other representative Re(108,110,120), the undulations behind the wake suggested the presence of unsteadiness.
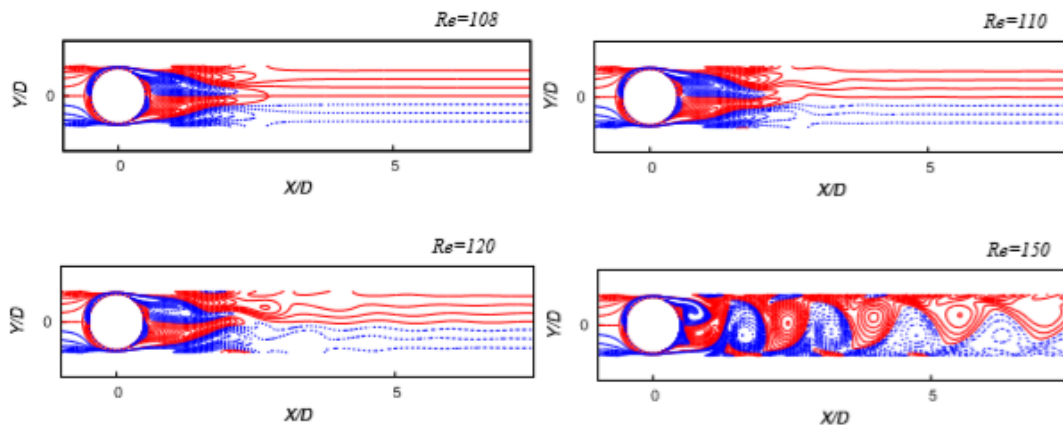
Sachin Saurabh

Figure 6: Vorticity contours for various Re (a) 108, (b) 110, (c) 120 and (d) 150.

5.4.2 Cd − Cl phase plot at Re= 150

For unsteady flow, it is observed that the phase portraits for drag and lift exhibits symmetry about the zerolift. The flow is also periodic over the unsteady regime. At Re = 150, the flow is periodic with multiple frequencies. The drag-lift phase portrait contains three crossover points and four loops at Re = 150.
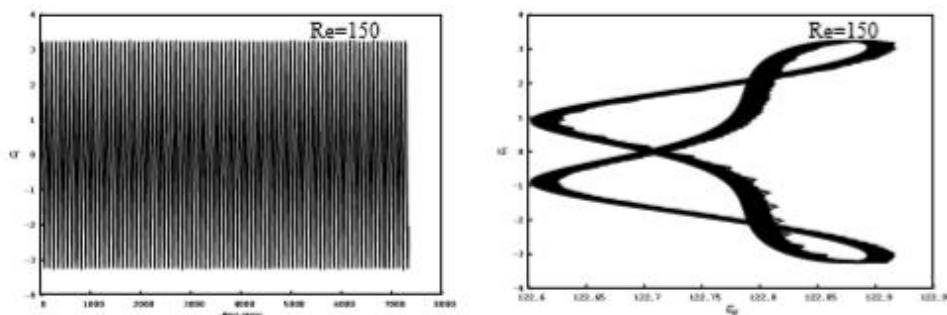

Figure 7: At $Re = 150$ (a) Time series of lift signal and (b) $C_d − C_l$ phase plot .

6 Conclusions

A stabilized finite element formulation using Streamline Upwind/Petrov Galerkin (SUPG) and Pressure stabilized/Petrov Galerkin (PSPG) method with great accuracy is used. A parabolic flow with no-slip boundary condition at lateral walls and stress free condition at downstream are used. It is observed that flow is symmetric about X-axis. Strong vortices appeared due to disturbance of wall resulting in high drag. The seperation appeared between the span of Re = 30 and 40. It is perhaps the first time that coefficient of pressure is

Sachin Saurabh

observed to be positive at rear stagnation point, Cpb. The minimum pressure coefficient remains positive upto Re = 80,followed by a small range of negative pressure is observed. The flow becomes unsteady after the critical value of 108. At Re = 150 strong vortex shedding is present. Due to high blockage the wall effect on vortex street behind the cylinder can be observed for Re more than 100.

References

[1] A. E. Hamielec and J. D. Raal. Numerical Studies of Viscous Flow around Circular Cylinders. Physics of Fluids , 12:1969.

[2] S. C. R. Dennis and G. Z. Chang. Numerical solutions for steady flow past a circular cylinder at reynolds numbers up to 100. Jornal of Fluids and Structures,42:471489,1970.

[3] M. Behr, D. Hastreiter, S. Mittal, T.E. Tezduyar. Icompressible flow past a circular cylinder: Dependence of the computed flow field on the location of the lateral boundaries. Methods in Applied Mechanics and Engineering, 123:309–316, 1994.

[4] Bhaskar Kumar and Sanjay Mitta. Effect of blockage on critical parameter for flow past over circular cylinder. Journal of Fluids and Structures,50:9871001,2006.

[5] Mehmet Sahin and Robert G. Owens. A numerical investigation of wall effects up to high blockage ratios on two-dimensional flow past a confined circular cylinder. LMF-ISE-FSTI, Ecole Polytechnique Fe de rale de Lausanne, CH 1015 Lausanne, Switzerland,16,2004.

[6] Jyoti Chakraborty, Nishith Verma, R.P. Chhabra. Wall effects in flow past a circular cylinder in a plane channel;Chemical Engineering and Processing. Chemical Engineering and Processing , 43:1529-1537,2004.

[7] Subhankar Sen, S .Mittal. Steady separated flow past a circular cylinder at low Reynolds numbers... J. Fluid Mech., vol. 620, pp.89119,2004.

[8] T. E. Tezduyar, M Behr, and J Liou. A new strategy for finite element computations involving moving boundaries and interfaces—the dsd/st procedure: I. the concept and the preliminary numerical tests. Comput.

Methods Appl. Mech. Eng., 94:339–351, 1992a.

[9] T. E. Tezduyar, M Behr, S Mittal, and J Liou. A new strategy for finite element computations involving moving boundaries and interfaces–the dsd/st procedure: II. computation of free-surface flows, two-liquid

flows, and flows with drifting cylinders. Comput. Methods Appl. Mech. Eng., 94:353–371, 1992b.

[10] S. Mittal and V. Kumar. Finite element study of vortex-induced cross-flow and in-line oscillations of a circular cylinder at low reynolds numbers. International Journal for Numerical Methods in Fluids, 31:1087–1120, 1999.

A Brief Author Biography

Sachin Saurabh– Presently working as a lecture in department of mechanical engineering,Assosa university Ethiopia M.tech(Spl in Thermal Engineering) From Indian Institute of Technology(ISM) Dhanbad and also having five years of teaching experience.My research area of interest is fluid mechanics and computational Fluid Dynamics(CFD) due to its various mode of solutions to solve realistic fluid flow problems.

Sachin Saurabh